Original Research Paper

High Resolution Satellite Images to Reconstruct Recent Evolution of Domitian Coastline

Pasquale Maglione, Claudio Parente and Andrea Vallario

Department of Sciences and Technologies,
University of Naples, "Parthenope", Centro Direzionale-Isola C4, Naples Italy

Corresponding Author:
Pasquale Maglione
Department of Sciences and
Technologies, University of
Naples "Parthenope", Centro
Direzionale-Isola C4, Naples
Italy
Tel.: +39-81-547-6597
Email: pasquale.maglione@uniparthenope.it

Abstract: In the last decades, combinations of natural and human factors have resulted in extensive morphological changes to our coastlines and in many cases have amplified erosion. In order to limit these changes and their impact on coastal zone, it is important to plan specific actions; for this purpose detailed cognizance of coastal zone is necessary. Different and heterogeneous data such as historical and recent maps, remotely sensed images and topographic survey result very useful to reconstruct temporal shoreline changes. In this study the attention is focalized on Domitian coastal zone (Italy), which is one of the most emblematic examples of coastal erosion in Europe. Study of the shoreline evolution in this area between 1876 and 2005 was used as the starting point of the present paper that investigates over a span of seven years (2005 to 2012), by using remotely sensed data. The aim is to adapt and integrate geomatics techniques to transform very high resolution satellite images in powerful tools to analyse coastline changes. So, in order to identify eroded and added areas, IKONOS-2 (2005), GeoEye-1 (2011) and WorldView-2 (2012) imageries are compared. These data-sets were re-georeferred to improve the positional accuracy. More over Normalized Difference Water Index (NDWI) was applied to pan-sharpened multispectral images to facilitate coastline vectorising at the same geometric resolution of panchromatic data. In addition, variance propagation was considered to establish the accuracy of the reconstruction of coastal evolution. Added and eroded areas were defined and related to the impact of the defence structures that were built in this zone in 2011.

Keywords: Coastline Changes, Remote Sensing, High Resolution Satellite Images, Geoinformatics, Digital Mapping, Positional Accuracy, Variance Propagation, Domitian Coastal Zone

Introduction

In the last decades natural factors (such as wind, near shore currents, sea level rise, vertical land movement) and human activities (such as coastal engineering, gas mining and water extraction, dredging, vegetation clearing) have resulted in erosion phenomena with the consequent decreasing in the extensions of many coastal zones (EC, 2004).

Coastline movement due to erosion and deposition is a major concern for coastal zone management. Very dynamic coastlines pose considerable hazards to human use and development and rapid replicable techniques are required to update coastline maps of these areas (White and Asmar, 1999).

To repair the damage and to mitigate the future impacts, phenomena models have to be prepared using all the available data, such as ancient and recent maps, air photos and satellite images, to reconstruct the evolution of the shoreline (Basile Giannini *et al.*, 2011). The repetitive acquisition and synoptic capabilities of remote sensing systems will provide timely spatial data for Geographical Information Systems (GIS), enabling detection and monitoring of coastline movement (White and Asmar, 1999).

Several studies about shoreline mapping and evolution have been carried out in the last years. Over this period, the use of optical satellite images for automatic and semi-automatic shoreline extraction has complemented the traditional approach based on surveying methods and air-photo processing. As a matter of fact, Frazier and Page (2000), used classification on Landsat 5 TM data to delineate water bodies on riverine

Science Publications

floodplains; similarly, Scott *et al*. (2003), adopted Landsat 7 ETM+ to extract land-water interface and generate shoreline data by Tasseled Cap Transformation coefficients derived by the EROS data. In these works medium resolution remotely images were used; in fact, in Lands at multispectral images pixel size is 30 m. In this case and for low resolution images, the definition of coastline as the intersection of land and water surfaces (Boak and Turner, 2005) can be usefully adopted: The different nature (and signature) of the two neighboring elements facilitates to detect and marks the limit between them. The launch of IKONOS in September 1999, Quick Bird in October 2001 and WorlView-2 in October 2009 marked the beginning of a new era. In fact, Very High Resolution (VHR) satellites are able to capture images of the earth's surface with a *Ground Sample Distance* (GSD) of 1 m or less (Aguilar *et al*., 2013). Chalabi *et al*. (2006), for example, considered IKONOS data set and aerial photographs to extract shoreline by segmentation technique and thresholds DN; Tarmizi *et al*. (2014), took into account several image classification methods such ISODATA to delineate the shoreline; Basile Giannini and Parente (2014) used object oriented approach to extract coastline from Quickbird imagery. In presence of very high resolution images two considerations are necessary. The first concerns the variability of coastline position in dependence of the moment of acquisition due to tidal fluctuations (Aguilar *et al*., 2010). The second regards geomorphologic units: For sandy beaches and wetlands, the coastline is the vegetation limit; for soft rock cliffs, it is the foot of the hillslope; for hard rock cliffs, the top of the cliff (Puissant *et al*., 2008).

In the present study, temporal series of VHR images were used to evaluate the shoreline evolution. According to other studies e.g., Maglione *et al*. (2014a), coastline detection was based on Normalized Difference Water Index (NDWI) resulting by Red and Near Infrared bands. To increase geometric resolution of the multispectral images, pan-sharpening approach was used; the line of separation between sea and land was performed applying Maximum Likelihood algorithm to NDWI image, so to obtain the threshold in empiric way. In addition, metric analysis to evaluate the accuracy of the eroded and added areas was carried out.

Study Area

The considered zone belongs to Campania coastal territory named Domitian littoral which delimits Campanian Plain (West), from Aurunci (North-West) to Lattari Mountains (South) and from Caserta (North) to Avella (North-East). Massive layers of alluvial materials from the Volturno River, as well as pyroclastic deposits of the Roccamonfina and Campi Flegrei volcanoes, have

contributed to fill a deep graben (Brancaccio *et al*., 1991). Inland, the beach shows at least two dune ridges, nearly parallel to the coastline; behind them extensive wetlands develop, where subsidence phenomena have recently occurred as a consequence of both natural and anthropogenic causes (De Pippo *et al*., 2008). Particularly, the considered coastline, approximately 1880 m long, is located in the territory of Castelvolturno Municipality (Fig. 1) and collected data cover a period from 2005 to 2012.

Sea currents and circulation that interest this area are well described in De Pippo *et al*. (2003). This zone is influenced by the circulation pattern of the Tyrrhenian Sea (Fig. 2) which confirms the presence of a cyclonic vortex that interests both the superficial (down to -10 m depth) and the intermediate (between -10 and -100 m depth) layers. In winter this type of circulation is more intense and moves from South along shelf break. The presence of the isle of Ischia obstacles this circulation and generate two secondary cells in correspondence to the Garigliano and Volturno river mouths (Fig. 2a). In summer the circulation moves from North and is characterized by reduced dynamics, but it preserves its cyclonic aspect and the water flow is influenced by the coastal morphology (Fig. 2b). The formation of secondary cells and offshore regime, dominated by the cyclonic gyre of the Tyrrhenian Sea, are responsible for sediment distribution.

Many studies starting from 1980 have analyzed the coastline variation in the observed territory (Cocco *et al*., 1984; 1994). Dynamic nature evolution of the shoreline is evident from analysis of historical maps conducted in a previous study that considered the evolution of this area from 1876 to 2005 (Basile Giannini *et al*., 2011). Particularly for the period from 1876 to 1984, cartographic products of Istituto Geografico Militare Italiano (IGM) in different scales (1:25000 or 1:50000) were used, while, from 1994 to 2005, both satellite and airplane remotely sensed images were taken into account.

According to this previous study (Fig. 3), it is possible to see that in the period from 1905 to 1954 a natural increase in the beach occurred; while between 1954 to 1984 more eroded and added areas were present. On the contrary, the eroding phenomena went on throughout the period 1984 to 2005, although with a slower impact in the last part of the examined span.

The main causes of erosion phenomenon of this area could be the alteration of the sedimentary cycles and the littoral dynamics and the modification of the coastal dunes; in 2011 to reduce these effects the following structures, in addition to environmental requalification, were built (Conte, 2011): one breakwater (artificial reef: Length is 890 m; distance from the shore is 170 m; mean distance from sea level is 0.50 m) parallel to the coastline and two groynes (length is 160 m) perpendicular to the coastline.
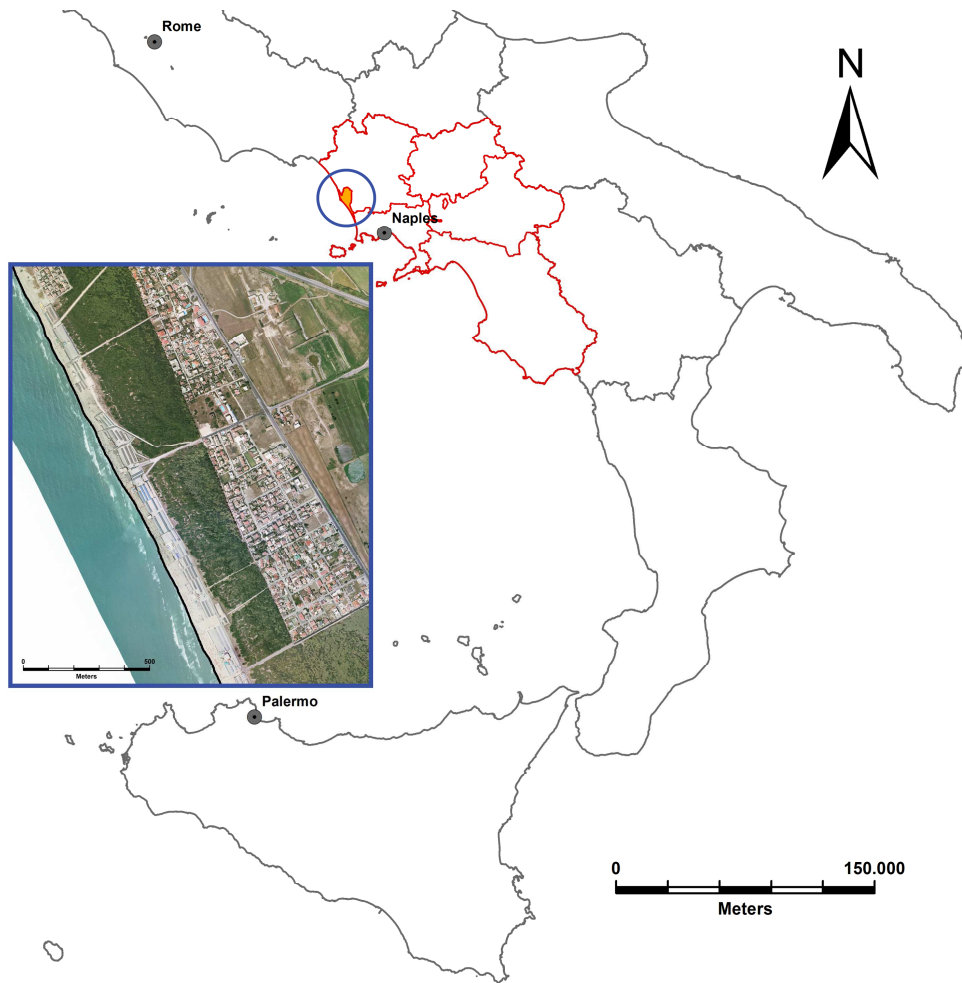
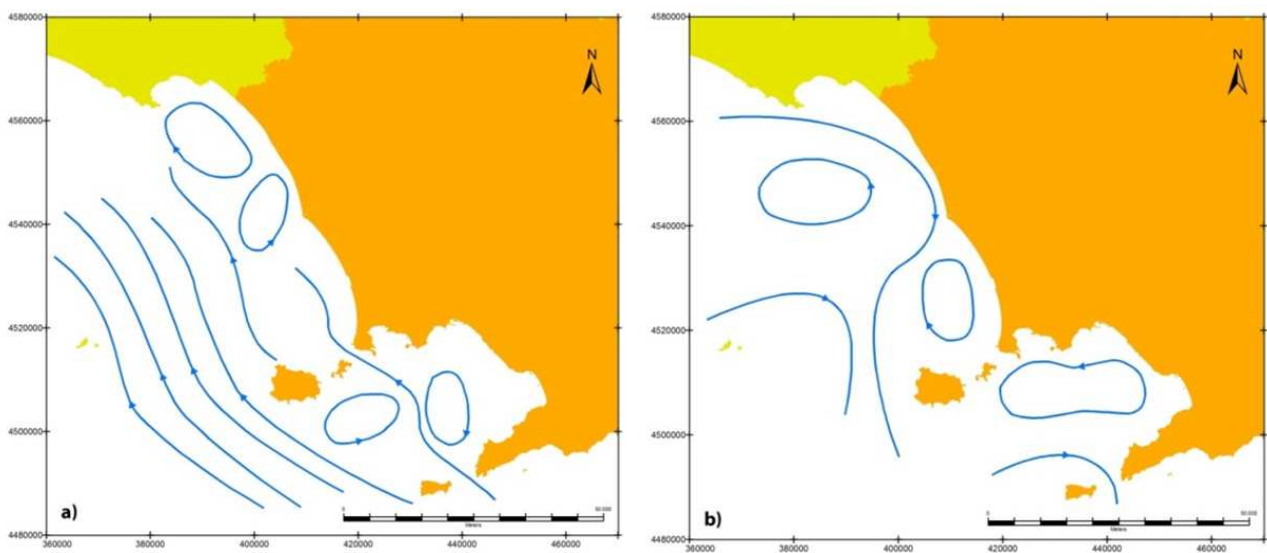Fig. 1. Territorial framework of the study area

Fig. 2. Circulation patterns of Tyrrhenian Sea in winter (a) and summer (b) (source: (DigitalGlobe, 2014)). The coordinates reported on the map are referred to UTM/ED50 and expressed in meters
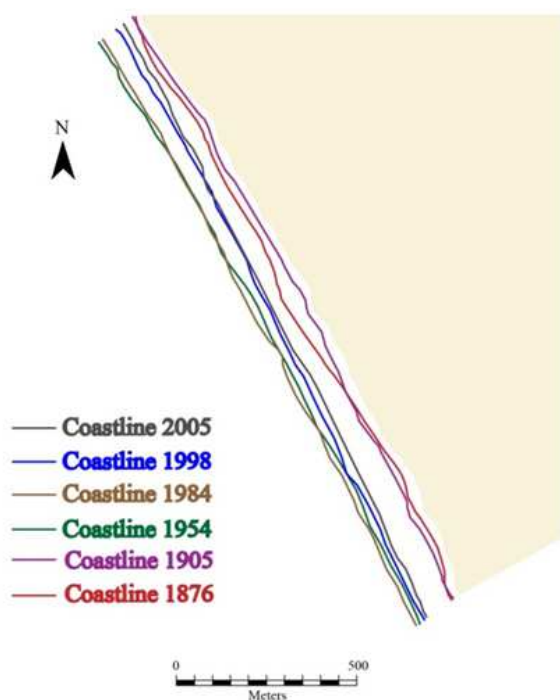
Fig. 3. Coastline evolution from 1876 to 200 (Basile Giannini *et al.*, 2011)

Hydrodynamic models had demonstrated that in absence of engineering opera coastline drew back of about 30-40 m in the following 20 years, so the decision to build the above mentioned structures was taken.

Data and Methods

Dataset and Early Elaboration

In this study three information sources concerning the Domitian coast at different date were considered: IKONOS-2 (2005), GeoEye-1 (2011) and WorldView-2 (2012) imagery.

IKONOS-2 dataset, acquired on 04/11/2005, included4 multispectral images (Blue: 0.445-0.516 µm; Green: 0.506-0.595 µm; Red: 0.632-0.698 µm; Near-Infrared: 0.757-0.853 µm) with pixel dimensions 4×4 m and 1 panchromatic image (0.450-0.900 µm) with cell size 1×1 m (Wang *et al.*, 2004).

GeoEye-1 dataset, acquired on 17/08/2011, included 4 multispectral images (Blue: 0.450-0.510 µm; Green: 0.510-0.580 µm; Red: 0.655-0.690 µm; Near-Infrared: 0.780-0.920 µm) with pixel dimensions 2.0×2.0 m and 1 panchromatic image (0.450-0.800 µm) with cell size 0.50×0.50 m (Geoimage, 2014).

WorldView-2 (WV-2) dataset, acquired on 10/08/2012, included 8 multispectral images (Coastal: 0.396-0.458 µm; Blue: 0.450-0.510 µm; Green: 0.510-0.580 µm; Yellow 0.585-0.625 µm, Red: 0.630-0.690

µm; Red-Edge 0.705-0.745 µm; NIR1 0.770-0.895 µm, NIR2 860-940 µm) with pixel dimensions 2.0×2.0 m and 1 panchromatic image (0.45-0.90 µm) with cell size 0.50×0.50 m (DigitalGlobe, 2014).

All images of the datasets listed above had been already orthorectified by using Rational Polynomial Functions (RPFs) (Maglione *et al.*, 2014b). The area under observation was extracted to be analysed. Initially, geographical location test was carried out by using 15 Check Points (CPs) which reference coordinates were deduced by orthophotos of Campania Region acquired on 2004 (nominal scale: 1:2.000; pixel dimensions 0.20 m) with identification by visiting (ground truthing), or by GNSS survey. Statistical characterizations of the residues (in meters) are reported in Table 1.

To improve the positional accuracy of the extracted area further rectification was applied to each dataset by means of OrthoEngine (PCI Geomatica) using Polynomial Functions (PFs) of 5th order (Errico *et al.*, 2009). This approach required for each scene almost 20 *Ground Control Points* (*GCPs*) easily detectable in the image and with known coordinates in a specific cartographic system. In this case 30 GCPs were used as well as 15 Check Points to evaluate accuracy of the georeferencing (cartographic system: UTM-WGS 84). To obtained the cartographic locations of these points the same above mentioned orthophotos as well as results of GNSS survey were used. Figures 4-6 show the distribution of both GCPs and CPs in each image. To limit acquisition errors, all points were selected for objects without problems of sunlight (above all corners of road junctions, corners of buildings, corners of swimming-pools, etc); examples of CPs and GCPs location are shown in Fig. 7.

In Table 2-4 are reported values of statistical characterizations of these residues.

Coastline Vectorising

The IKONOS 2 imagery was acquired before the defense structures construction. The groins are evident in the other two datasets (GeoEye-1 and WordView-2) while the breakwater is less manifest because under water (its shape can be enhanced using RGB composition).

For each imagery the wet-dry line was used as instantaneous coastline (Li *et al.*, 2002; Tarig Abdelgayoum, 2003) and a manual vectoring was applied to trace it. To better distinguish the limit between the sea and the sandy beach, so to support the operator in this manual operation, Normalized Difference Water Index (NDWI)–(Wolf, 2010) was applied:

$$NDWI = \frac{Blue - NIR}{Blue + NIR} \tag{1}$$

Table 1. Statistical characterizations of residues (in meters) calculated for 15 CPs on the original orthorectified images

15 CPs	Mean (m)	Min (m)	Max (m)	σ (m)	RMS (m)
Ikonos-2	1.406	0.280	3.677	0.845	1.640
GeoEye-1	0.891	0.136	2.600	0.591	1.069
WV-2	0.945	0.007	2.670	0.738	1.199

Table 2. Statistical characterizations of residues (in meters) obtained for 30 GCPs and 15 CPs with application of PFs (5th order) to the IKONOS-2 imagery

	Mean (m)	Min (m)	Max (m)	σ (m)	RMS (m)
GCPs (30)	0.656	0.038	1.615	0.439	0.789
CPs (15)	1.083	0.125	1.831	0.497	1.192

Table 3. Statistical characterizations of residues (in meters) obtained for 30 GCPs and 15 CPs with application of PFs (5th order) tothe GeoEye-1 imagery

	Mean (m)	Min (m)	Max (m)	σ (m)	RMS (m)
GCPs (30)	0.302	0.011	0.676	0.302	0.427
CPs (15)	0.648	0.119	1.238	0.288	0.709

Table 4. Statistical characterizations of residues (in meters) obtained for 30 GCPs and 15 CPs with application of PFs (5th order) to the WorldView-2 imagery

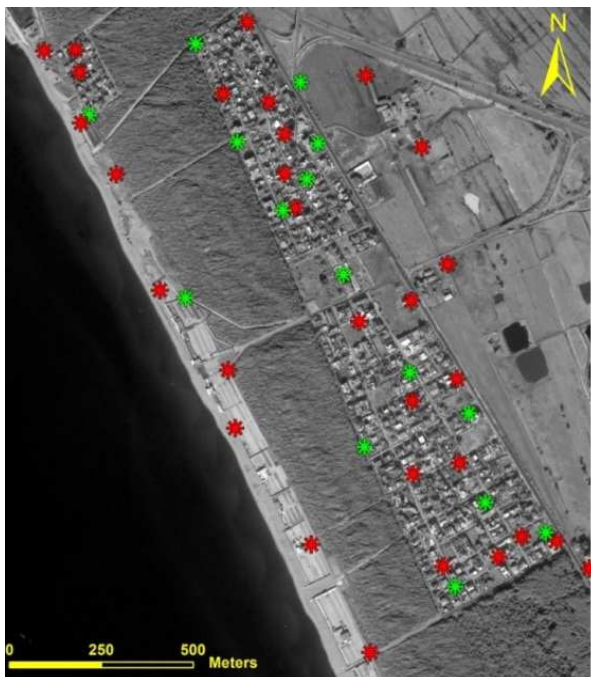|	Mean (m)	Min (m)	Max (m)	σ (m)	RMS (m)
GCPs (30)	0.260	0.002	0.641	0.202	0.329
CPs (15)	0.597	0.182	0.932	0.239	0.643

Fig. 4. Rectification of the IKONOS-2 imagery: Location of 30 GCPs (in red) and 15 CPs (in green)
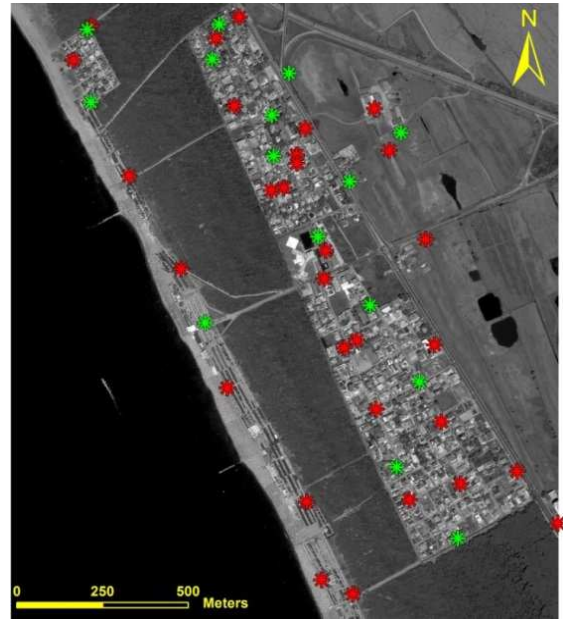

Fig. 5. Rectification of the GeoEye-1 imagery: Location of 30 GCPs (in red) and 15 CPs (in green)
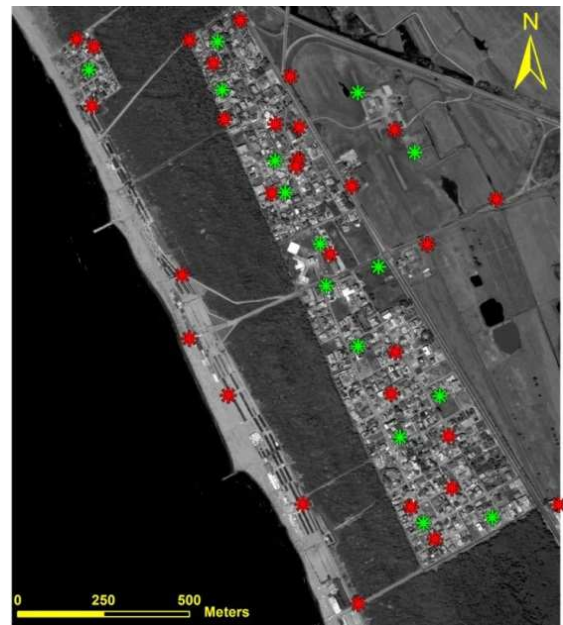

Fig. 6. Rectification of the WorldView-2 imagery: Location of 30 GCPs (in red) and 15 CPs (in green)

Introduced in 1996 by McFeeters (1996) to difference land surface water and vegetation in Land sat TM images, NDWI was then modified by Xu (2006) that changed the combination of the bands to distinguish water from bare soil. The theoretical values of this index are between -1 and 1: As it is easy to deduce taking into account the spectral signatures, vegetation is characterized by low values, the water presents rather high values and the soil is placed in the middle position of the interval (Fig. 8).
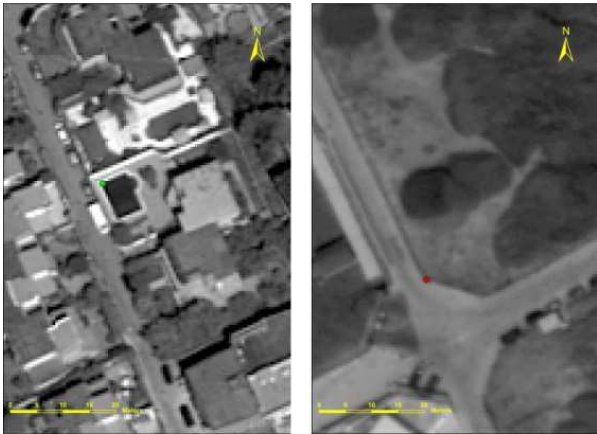
Fig. 7. Examples of CP (in green) on the GeoEye-1 panchromatic image (on the left) and GCP (in red) on the WorldView-2 one (on the right)

Fig. 8. NDWI resulting from WorldView-2 imagery

(a)   (b)

Fig. 9. Pansharpening application to WorldView-2: (a) detail of RGB composition of original multispectral images; (b) detail of RGB composition of pan-sharpened multispectral images

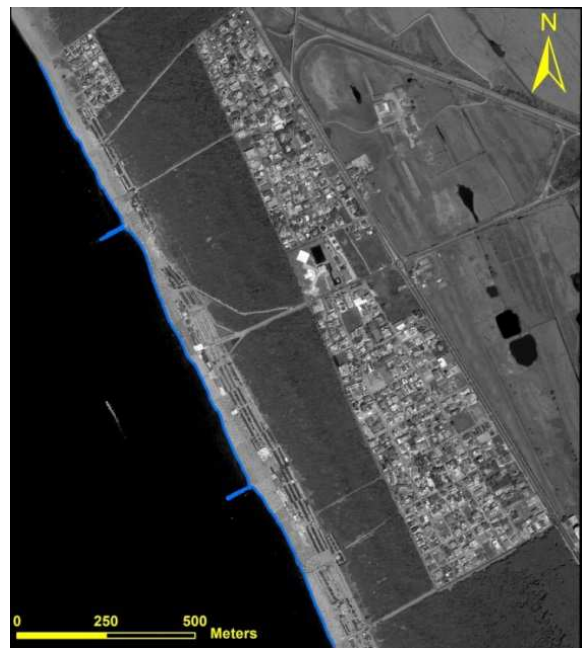Fig. 10. Vector coastline on IKONOS-2 panchromatic image

Fig. 11. Vector coastline on GeoEye-1 panchromatic image

Because of the lower geometric resolution of multispectral data, pan-sharpening (Vrabel, 2000; Yang *et al*., 2010; Parente and Santamaria, 2013; 2014) was applied to reduce pixel dimensions. A large number of pan-sharpening methods are present in the literature of the last two decades: One of them named Zhang method (Zhang, 1999) and implemented in the software Focus by PCI Geomatics Enterprise, was applied in this study because of its considerable level of performance.
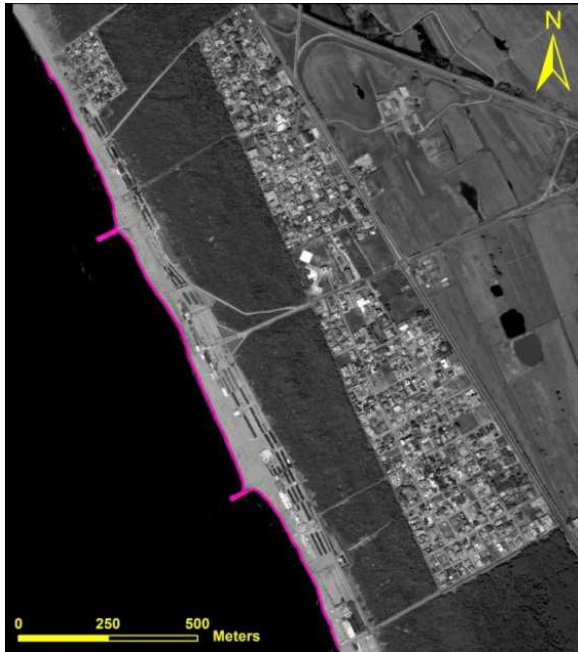
Fig. 12. Vector coastline on WorldView-2 panchromatic image

In this way the geometric resolution of the panchromatic data was transferred to multispectral ones (Fig. 9) and more detailed images were derived (for example, pixel dimension of multispectral data was conducted from 2 to 0.5 m in the cases of WorldView-2 and GeoEye-1). NDWI maps were classified so distinguishing wet and dry pixels. Particularly, the same training sites were used for each dataset and Maximum Likelihood algorithm was applied. The resulting NDWI maps in combination with panchromatic layers were used to support the vectorisation of the coastline (Fig. 10-12).

Results and Discussion

To reconstruct and analyse shoreline evolution 2 pairs of temporally consecutive coastlines were considered; for each temporal interval the eroded and added areas were calculated and metric accuracy of those values established (Fig. 13 and 14).

Primarily metric positional accuracy of each coastline was recognized considering the uncertainty that characterized it: about horizontal position two types of errors, the first related to the images, the second to the tides effects, were evaluated. The former was due to the geometric resolution of the satellite data and georeferencing operations, so pixel dimensions and xy residues reported in section "*Data Set and Early Elaboration*" were used to calculated it.

The hydrometric level data were considered to evaluate errors related to the tide effects. These data were obtained from ISPRA website (Istituto Superiore per la Protezione e la Ricerca Ambientale) (ISPRA, 2014) for the acquisition time of each image (that was reported in metadata file).
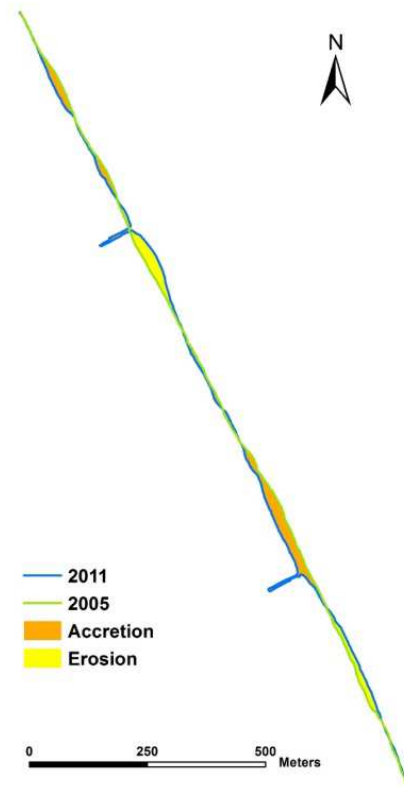

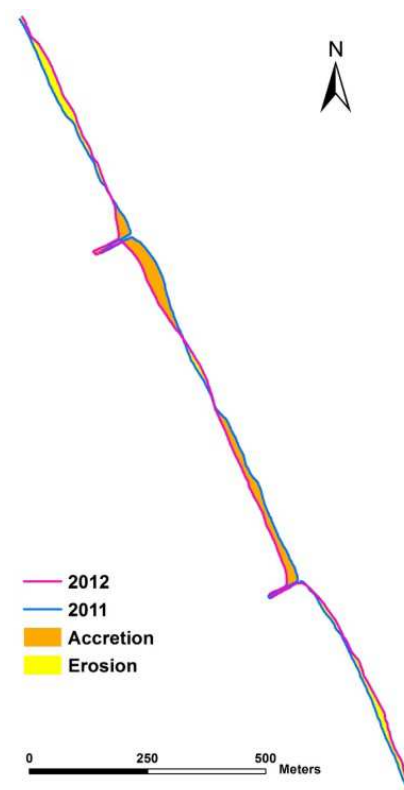
Fig. 13. Shoreline evolution between 2005-2011

Fig. 14. Shoreline evolution between 2011-2012

The collected data were referred to the tide gauge in the port area of Gaeta for the 2011 and 2012 and Naples for 2005. Gaeta was chosen because it is nearest to the investigated zone; for 2005 the port area of Naples was considered because of the absence of hydrometric level data on Gaeta concerning this year.

The resulted hydrometric level data are reported in Table 5.

To define uncertainty relative to tides, slope was necessary. Of course the exact incline values related to the acquisition time of each image and to the horizontal position of each point of the coastline were not available. For consequence, in consideration of different surveys that were carried out in this zone starting from 2003 (Carnevale, 2003), a constant slope (15%) from beach to sea was considered. The resulted values of the errors for each coastline due to tide effects are reported in Table 6: In consideration of the exposure of the beach, raising of the water level produced coastline shifting from South-West to North-East, sinking from North-East to South-West.

To define metric positional accuracy of each coastline the well known formula of propagation of variance for linear case was applied (Cina, 2002):

$$\sigma_y^2 = \sum_{i=1}^{n} \sigma_i^2 \tag{2}$$

where, σ_i^2 was supplied by each horizontal position error above illustrated.

Propagation of variance for non-linear case was applied to eroded and added areas calculation (Cina, 2002):

$$\sigma_A^2 = b^2 \bullet \sigma_a^2 + a^2 \bullet \sigma_b^2 \tag{3}$$

Where:
a and b = The sides of the rectangle that approximated the area between the considered coastlines (their values were established preserving the same ratio between the lengths of the respective coastlines)
σ_a and σ_b = The horizontal position errors about the considered coastlines

The results are shown in Table 7.

The index "I" was considered to evaluate the average shift between two temporal consecutive shorelines (Guastaferro *et al.*, 2011):

$$I = \frac{S}{L} \tag{4}$$

Where:
S = The total area of the eroded (or added) polygons
L = The length of the relative coastline taken as reference (the older coastline in each interval)

The values of this index for each temporal range and for both eroded and added areas are shown in Table 8.

Table 5. The considered hydrometric values

Year	Port area	Hydrometric value (m)
2005	Naples	-0.10
2011	Gaeta	0.05
2012	Gaeta	-0.10

Table 6. Planimetric errors relative to tides

Year	Errors (m)
2005	0.67
2011	0.33
2012	0.67

Table 7. Eroded and added areas for each time period

Period	Eroded Area (m^2)	Added Area (m^2)
2005-2011	6611±116	10052±155
2011-2012	9560±103	12918±121

Table 8. I index for each time period

Time period	Eroded (m)	Added (m)
2005-2011	8.113	7.399
2011-2012	8.082	13.944

The comparison between coastlines 2005-2011 evidenced the early effects of the human intervention to limit erosion phenomena: groyes and breakwater imposed physical barriers in the near shore zone and tended to block the flow of littoral drift. This tendency is remarked by the shoreline evolution between 2011-2012: Groins trap materials moving parallel to the shore producing accretion in the intern zone while supply of materials to down drift beaches was reduced, so downstream erosion was accelerated.

Conclusion

Two basic types of conclusions can be derived from this application, one concerning methodological aspects, the other the evolutionary process of the Domitian coast. In reference to the first, availability of high-resolution remotely sensed images can provide useful data for the reconstruction of coastal dynamics. Considering the accuracy of different information sources and the law of propagation of variance, quantitative analysis of the erosion magnitude and reconstruction of the evolutionary framework are possible. The working environment consists of the most useful GIS. Acceptable quality level of overlapping is possible using geometric transformations based on Ground Control Points which coordinates can be obtained either directly from maps, topographic survey or already georeferenced images (orthophotos).

Regarding evolutionary aspects of the Domitian coast in the last decade, this study remarks the effects that were generated because of the introduction of two groins and one breakwater in 2011 to interrupt water flow and limit movement of sediments. In fact the comparison of IKONOS (2005), Geo-Eye (2011) and WorldView-2

(2012) imageries evidences the contemporary presence of eroded parts and added ones: The effects of the barrier system are manifest because of the accretion of materials in the intern zone (between the groins), but also the removal of sands from nearby down drift beaches.

Acknowledgment

Funding Information

Author's Contributions

This paper is the result of the full and equal collaboration of all the authors.

Ethics

The authors have not conflicts of interest in the development and publication of this paper.

References

Aguilar, F.J., I. Fernández, J.L. Pérez, A. López and M.A. Aguilar *et al.*, 2010. Preliminary results on high accuracy estimation of shoreline change rate based on coastal elevation models. Int. Archives Photogrammetry, Remote Sensing Spatial Inform. Sci., 33: 986-991.

Aguilar, M.A., M.M. Saldaña and F.J. Aguilar, 2013. GeoEye-1 and WorldView-2 pan-sharpened imagery for object-based classification in urban environments. Int. J. Remote Sensing, 34: 2583-2606. DOI: 10.1080/01431161.2012.747018

Basile Giannini, M. and C. Parente, 2014. An object based approach for coastline extraction from Quickbird multispectral images. Int. J. Eng. Technol., 6: 2698-2704.

Basile Giannini, M., P. Maglione, C. Parente and R. Santamaria, 2011. Cartography and Remote sensing for coastal erosion analysis. Proceedings of the Coastal Process II, Apr. 27-29, Naples, Italy, WIT Press, pp: 65-76. DOI: 10.2495/CP110061

Boak, E.H. and I.L. Turner, 2005. Shoreline definition and detection: A review. J. Coastal Res., 21: 688-703. DOI: 10.2112/03-0071.1

Brancaccio, L., A. Cinque, P. Romano, C. Rosskopf and F. Russo *et al.*, 1991. Geomorphology and neotectonic evolution of a sector of the Tyrrhenian flank of the Southern Apennines (Region of Naples, Italy). Zeitschrift fur Geomorphologie, Supplementbande, 82: 47-58.

Carnevale, L., 2003. Applicazioni GIS per indagini relative all'evoluzione della linea di costa. PhD Thesis, University of Naples "Parthenope".

Chalabi, A., H. Mohd-Lokman, I. Mohd-Suffian, M. Karamali and V. Arthigeyan *et al.*, 2006. Monitoring shoreline change using IKONOS image and aerial photographs: A case study ok Kuala Terengganu area, Malaysia. Enschede, Netherlands.

Cina, A., 2002. Trattamento Delle Misure Topografiche: Teoria Ed Esercizi. 2nd Edn., Celid, Torino, ISBN-10: 8876615342, pp: 125.

Cocco, E., M.A. De Magistris and Y. Iacono, 1994. Modificazioni dell'ambiente costiero in Campania (Litorale Domizio, Golfo di Gaeta) in conseguenza delle opere umane. Il Quaterario-Italian J. Quaternary Sci., 7: 409-414.

Cocco, E., M.A. De Magistris, T. De Pippo and A. Perna, 1984. Dinamica ed evoluzione del litorale campano-laziale: 3. Il complesso di foce del fiume Volturno. Proceedings of the VI Congresso A.I.O.L., Livorno, Italy.

Conte, D., 2011. L'impiego della modellistica numerica e fisica nello studio dell'efficacia e dell'impatto di un'opera di difesa costiera: La scogliera soffolta di Ischitella. Proceedings of Italian DHI Conference, Oct. 11-12, Torino, Italy.

De Pippo, T., C. Donadio and M. Pennetta, 2003. Morphological control on sediment dispersal along the southern Tyrrhenian coastal zones (Italy). Geologica Romana, 37: 113-121.

De Pippo, T., C. Donadio, M. Pennetta, C. Petrosino and F. Terlizzi *et al.*, 2008. Coastal hazard assessment and mapping in Northern Campania. Geomorphology, 97: 451-466. DOI: 10.1016/j.geomorph.2007.08.015

DigitalGlobe, 2014. http://www.digitalglobe.com/sites/default/files/Basic Imagery-DS-BASIC-PROD.PDF

Errico, A., P. Maglione, C. Parente and R. Santamaria, 2009. Impiego di immagini telerilevate da satellite per la produzione e l'aggiornamento di cartografia. Proceedings of the 13° Conferenza Nazionale ASITA, Bari, Italy, pp: 1012-1013.

EC, 2004. Living with coastal erosion in Europe–results from the eurosion study. Office for Official Publications of the European Communities, Netherlands.

Frazier, P.S. and K.J. Page, 2000. Water body detection and delineation with Landsat TM data. Photogrammetric Eng., Remote Sens., 66: 1461-1467.

Geoimage, 2014. http://launch.geoeye.com/LaunchSite/assets/documents/geoeye1_factsheet_v8.pdf

Guastaferro, F., P. Maglione, C. Parente and R. Santamaria, 2011. Estrazione in automatico della linea di costa da immagini satellitari IKONOS. Proceedings of the Conference Geomatica Le radici del futuro Tributo a Sergio Degual and Riccardo Galetto. Feb. 10-11, Pavia, Italy, pp: 109-116.

ISPRA, 2014. La rete mareografica nazionale. Istituto Superiore per la Protezione e la Ricerca Ambientale.

Li, R., R. Ma and K. Di, 2002. Digital tide-coordinated shorelines. Marine Geodesy, 25: 27-36. DOI: 10.1080/014904102753516714

Maglione, P., C. Parente and A. Vallario, 2014a. Coastline extraction using high resolution WorldView-2 satellite imagery. Eur. J. Remote Sens., 47: 685-699. DOI: 10.5721/EuJRS20144739

Maglione, P., C. Parente, R. Santamaria and A. Vallario, 2014b. Modelli tematici 3D della copertura del suolo a partire da DTM e immagini telerilevate ad alta risoluzione WorldView-2. Rendiconti Online della Società Geologica Italiana, 30: 33-40. DOI: 10.3301/ROL.2014.08

McFeeters, S.K., 1996. The use of the Normalized Difference Water Index (NDWI) in the delineation of open water features. Int. J. Remote Sens., 17: 1425-1432. DOI: 10.1080/01431169608948714

Parente, C. and R. Santamaria, 2013. Increasing geometric resolution of data supplied by quickbird multispectral sensors. Sensors Transducers, 156: 111-115.

Parente, C. and R. Santamaria, 2014. Synthetic sensor of landsat 7 ETM+ imagery to compare and evaluate pan-sharpening methods. Sensors Transducers, 177: 294-301.

Puissant, A., S. Lefèvre and J. Weber, 2008. Coastline extraction in VHR imagery using mathematical morphology with spatial and spectral knowledge. Proceedings of The 21st Congress of International Society of Photogrammetry and Remote Sensing, Beijing, Chine, pp: 1305-1310.

Scott, J.W., L.R. Moore, W.M. Harris and M.D. Reed, 2003. Using the landsat 7 enhanced thematic mapper tasseled cap transformation to extract shoreline. U.S. Geological Survey.

Tarig Abdelgayoum, A., 2003. New methods for positional quality assessment and change analysis of shoreline features. PhD Thesis, the Ohio State University.

Tarmizi, N.M., A.M. Samad and M.S.M. Yusop, 2014. Shoreline data extraction from QuickBird satellite image using semi-automatic technique. Proceedings of the 10th International Colloquium on Signal Processing and its Application, Mar. 7-9, Kuala Lumpur, Malaysia, pp: 157-162. DOI: 10.1109/CSPA.2014.6805739

Vrabel, J., 2000. Multi-spectral imagery advanced band sharpening study. Photogrammetric Eng. Remote Sens., 66: 73-79.

Wang, L., W.P. Sousa, P. Gong and G. Biging, 2004. Comparison of IKONOS and QuickBird images for mapping mangrove species on the Caribbean coast of Panama. Remote Sens. Environ., 91: 432-440. DOI: 10.1016/j.rse.2004.04.005

White, K. and H.M. El Asmar, 1999. Monitoring changing position of coastlines using Thematic Mapper imagery, an example from the Nile Delta. Geomorphology, 29: 93-105. DOI: 10.1016/S0169-555X(99)00008-2

Wolf, A., 2010. Using WorldView 2 Vis-NIR MSI imagery to support land mapping and feature extraction using normalized difference index ratios. Proceedings of the DigitalGlobe 8-Band Research Challenge, Longmont, Colorado (USA), pp: 1-13.

Xu, H.Q., 2006. Modification of Normalised Difference Water Index (NDWI) to enhance open water features in remotely sensed imagery. Int. J. Remote Sens., 27: 3025-3033. DOI: 10.1080/01431160600589179

Yang, J., J. Zhang, H. Li, Y. Sun and P. Pu, 2010. Pixel level fusion methods for remote sensing images: A current review. Proceedings of the ISPRS TC VII Symposium-100 Years ISPRS, Jul. 5-7, Vienna, Austria, pp: 680-686.

Zhang, Y., 1999. A new merging method and its spectral and spatial effects. Int. J. Remote Sens., 20: 2003-2014. DOI: 10.1080/014311699212317